Energy & Environmental Science

Cite this: *Energy Environ. Sci.*, 2011, **4**, 3420

www.rsc.org/ees

PAPER

Detachment and transfer of ordered TiO_2 nanotube arrays for front-illuminated dye-sensitized solar cells†

Lu-Lin Li, Yi-Ju Chen, Hui-Ping Wu, Niann S. Wang and Eric Wei-Guang Diau*

Received 24th September 2010, Accepted 10th May 2011
DOI: 10.1039/c0ee00474j

We report a method of detachment and transfer of one-dimensional TiO_2 nanotube (NT) arrays to fabricate dye-sensitized solar cells (DSSCs) with illumination from the front side. The ordered NT arrays (tube length 20 μm) were detached from the NT–Ti substrate, as annealed, by means of a second anodization at 20 V for 4 h and then transferred, inverted, onto a transparent substrate of conducting oxide (TCO) with an interface of TiO_2 nanoparticles of thickness ~2 μm. Dry etching of the NT surface in a highly dense plasma reactor under BCl_3/Cl_2 for 90 s opened previously closed ends of the tubes. The inverted (bottom-up) NT–TCO substrate was fabricated into a DSSC device that shows a cell performance ($\eta = 6.24\%$) significantly improved over those of a front-illuminated counterpart with an upright (face-up) structure ($\eta = 4.84\%$) and of a conventional back-illuminated device ($\eta = 4.61\%$). Electrochemical impedance spectra (EIS) of the devices under one-sun irradiation were measured to rationalize the cell performances that are consistent with the corresponding interfacial impedances between the NT arrays and the electrode for collection of electrons.

Introduction

The development of dye-sensitized solar cells (DSSCs) has introduced a possibility of obtaining cheap and efficient renewable energy from sunlight since 1991.[1] The photoanodes of DSSCs are composed typically of randomly packed, crystalline, TiO_2 nanoparticles (NP); the cell efficiency (η) of a NP-DSSC device has attained ~11%.[2–6] The development of photoanode materials that can accept injected electrons from the dyes and transport electrons to the charge-collection electrodes has received much attention due to their prominent effect on the efficiency of power conversion. To improve the cell performance, the following properties for the development of photoanode materials are considered important: a large surface area to facilitate light harvesting, comparable energy levels between the dye and electrolyte to facilitate electron injection and dye regeneration, and rapid transport of electrons and slow charge recombination of electrons to facilitate charge collection. For this purpose, well ordered one-dimensional nanostructures, such as TiO_2 nanotubes (NTs),[7–10] nanowires,[11] nanorods,[12,13] become effective candidates for photoanode materials because of their superior electron transport and small rate of charge recombination relative to a conventional NP-based system.[14]

Titania nanotubes, as vertically oriented arrays, have been prepared using potentiostatic anodization as a promising advance in DSSC applications. In addition to the great efficiency

Department of Applied Chemistry and Institute of Molecular Science, National Chiao Tung University, No. 1001, Ta Hsueh Rd., Hsinchu, 30050, Taiwan. E-mail: diau@mail.nctu.edu.tw; Fax: +886 03 572 3764

† This article was submitted as part of an issue highlighting papers from the International Conference on Ordered 1-Dimensional Nanostructures for Photovoltaics, held in September 2010.

Broader context

Dye-sensitized solar cells (DSSCs) are good candidates as clean, efficient, and low-cost energy conversion devices for the development of sustainable energy resources. In DSSCs, charge recombination in the dye/TiO_2 interface and electron transport at the photoanodes are the two important factors to be considered for promoting the efficiency of charge collection of the device. Vertically oriented one-dimensional titania nanotube (NT) arrays, fabricated by anodization, are promising photoanode materials for DSSCs due to their superior electron transport and small rate of charge recombination compared to a conventional nanoparticle system. In this article, we report a method of detachment and transfer of TiO_2 NT arrays onto a transparent conducting oxide (TCO) substrate for the device with a front-illuminated structure to improve the cell performance. The new approaches include detachment *via* a secondary anodization, transfer in an inverted manner, and dry etching to open the closed ends of the NT arrays, which are feasible to be applied for large scale front-illuminated NT-based DSSCs with high performance.

of charge collection and slow recombination of charge,[14] these titania NT arrays feature excellent intrinsic light scattering to harvest sunlight toward longer wavelengths.[14,15] The cell performances of the corresponding NT-DSSC devices have been promoted to $\eta = 7.6\%$ for a tube length 30 μm with a $TiCl_4$ post-treatment to increase the surface area.[15]

Even though a NT-based DSSC possesses the advantages specified above, a traditional NT-DSSC device based on illumination of the back side suffers degradation of performance because some incident light is absorbed by the iodide/tri-iodide electrolyte and scattered by the Pt-coated counter electrode. To improve the cell performance for a NT-DSSC device, transparent nanotube arrays were fabricated on a transparent conducting oxide (TCO) substrate using methods such as sputtering and anodization,[16–18] film detachment and transfer[19–23] or through a removable template.[24] For instance, using sputtering and anodization Grimes and co-workers prepared an efficient transparent NT-DSSC device ($\eta = 6.9\%$) with a tube length 17.6 μm that generated a titanium film of thickness 20 μm with a deposition period of 61 h.[18] The major challenge in the fabrication of transparent NT arrays with this method is the length of the nanotubes, which is limited by the thickness of the sputtered titanium film; the poor adhesion between the substrate and the titanium film becomes a further major problem to be resolved.

Park and co-workers reported the fabrication of transparent NT arrays obtained on detaching the NT film from a Ti foil in a HCl solution and transferring it to a TCO glass. The corresponding NT-DSSC device yields a conversion efficiency 7.6% after $TiCl_4$ post-treatment.[19] Chien and co-workers reported that the opened-end NT arrays can be served as an efficient transparent photoanode for NT-DSSC by peeling off the Ti substrate in an H_2O_2 solution and removing the bottom caps in an oxalic acid solution.[22] However, there are inherent problems with the wet chemical etching techniques mentioned above. One is that wet chemical etching, using either HCl,[19] CH_3OH/Br_2[25] or oxalic acid solution[26] to detach the NT film from the substrate and to open the closed bottom end of the tubes, is an isotropic etching treatment, which might result in the destruction of the nanotubes.[22,27] Another problem is that the existence of an interface, created by titanium alkoxide solution or titania NP paste to fix the NT arrays onto glass, might lead to a retarded electron transport to diminish the cell performance.[18,22] A third problem is the formation of cracks on the surface of the NT film and formation of a curled film that might limit the size of the device for future applications.

Here we report the use of detachment and transfer to fabricate strongly adhering, transparent NT arrays on a TCO glass for front-illuminated NT-DSSC. The procedure to detach the NT film from a Ti foil and transferring it onto a TCO glass is presented schematically in Fig. 1. Four steps in this method involve growth of an amorphous titania layer between NT arrays as prepared and the Ti foil through a secondary anodization process, detachment of the NT film from the Ti foil with an ultrasonic treatment, transfer and attachment of the inverted NT arrays onto FTO glass coated with a thin layer of TiO_2 NP paste, and opening the closed-end NT arrays with dry etching. In contrast to the isotropic wet chemical approach, our methods provide an anisotropic treatment to detach the NT arrays from the Ti substrate through the secondary anodization, and to open the closed-end NT arrays in the vertical direction *via* the dry etching process,[28] so that the possible destruction of the nanotubes can be avoided. The NT-DSSC device prepared with this approach achieved an efficiency ($\eta = 6.24\%$) of power conversion that significantly exceeds that of its front-illuminated counterpart fabricated with a conventional upright approach under the same conditions ($\eta = 4.84\%$).

Experimental

Fabrication of NT arrays

The titanium oxide nanotube arrays were fabricated with a standard anodization method.[8,15] Ti foil (commercially pure grade 1, purity 99.9%, substrate size 6 × 6 cm^2, Kobe steel) served as anode to grow NT arrays with another Ti foil of the same size as cathode. The ordered NT films were produced in electrolyte solutions containing ammonium fluoride (NH_4F, 99.9%, 0.4 mass%) in EG in the presence of H_2O (2 vol%) at 60 V for 8 h at 25 °C. The sample as anodized was washed in ethanol, and annealed at 450 °C for 1 h to crystallize amorphous TiO_2 into an anatase crystalline phase.[29] To remove the debris on the surface of the tubes, we treated the sample with ultrasonic agitation in ethanol for 15 min.

Detachment and transfer of NT arrays onto FTO substrate

The NT array film as prepared was detached with a second anodization[20] at bias voltages of 10, 20 and 25 V for 4 h in the same anodic electrolyte solution. After being washed with ethanol, the NT array film was detached from the Ti substrate. TiO_2 nanoparticles were prepared with a sol–gel method.[30] A paste composed of TiO_2 NP with particle size ~20 nm was coated by screen printing on a $TiCl_4$-pretreated FTO glass (15 Ω $\square^{-1}$) to obtain a film of thickness 2 μm. The detached NT arrays were transferred onto the FTO substrate with the TiO_2 NP paste as an interface; the direction of the attached NT arrays was either upright or inverted. The attached NT-FTO films were annealed in two steps: the films were first annealed at 150 °C for 0.5 h with temperature increasing at a rate of 2.5 °C min^{-1} to evaporate the organic solvents followed by annealing at 450 °C for 1 h with temperature increasing at a rate 5 °C min^{-1}. With this thermal treatment, the interfacial amorphous TiO_2 NP layer became crystallized into an anatase phase and the NT array film firmly adhered to the FTO glass. For the inverted approach, the closed tubes on top of the NT film were opened with dry etching in a highly dense plasma reactor under BCl_3/Cl_2 for periods 0–300 s. The surface morphology of the NT arrays was determined with a scanning electron microscope (SEM, JSM-6500F JEOL).

$TiCl_4$ post-treatment

The NT films were treated with $TiCl_4$ in two stages.[8] The films as prepared were first immersed in $TiCl_4$ solution (0.073 M) for 30 min followed by rinsing and drying near 23 °C. The films were re-immersed in $TiCl_4$ stock solution for 1 h and annealed at 350 °C for 30 min.

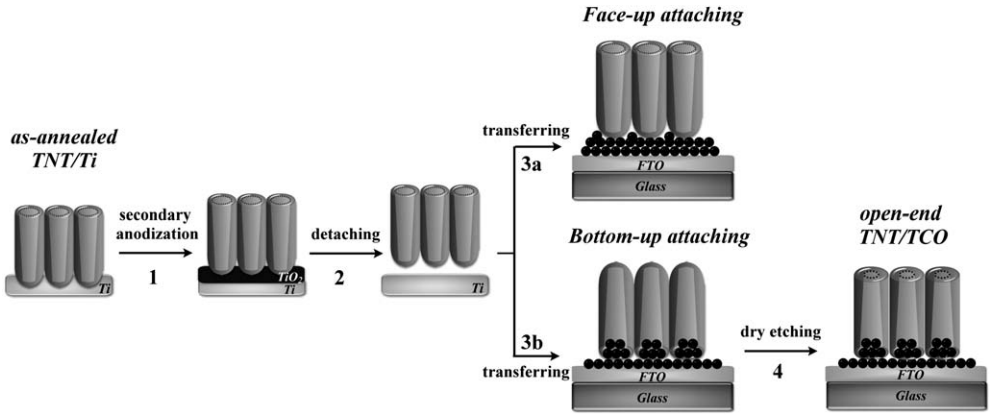

Fig. 1 Schematic representation of the detachment and transfer of the ordered 1D nanotube arrays for front-illuminated dye-sensitized solar cells.

Device fabrication

The trimmed TNT films (size 0.4 × 0.4 cm^2) were sensitized in a solution of N719 dye (Solaronix, 3 × 10^{-4} M) containing chenodeoxycholic acid (CDCA, 3 × 10^{-4} M) in acetonitrile/*tert*-butanol (v/v = 1 : 1) binary solvent for 18 h to absorb sufficient dye for light harvesting. After washing with ethanol, the N719/NT films were assembled with a transparent Pt-coated counter electrode that served as a cathode. The cathode was made on spin-coating a H_2PtCl_6/isopropanol solution on an indium-doped tin-oxide (ITO, 2.8 Ω $\square^{-1}$) glass substrate through thermal decomposition at 380 °C for 30 min.[31] The NT-DSSC device was sealed with a molten film (SX1170, Solaronix, thickness 25 μm); a thin layer of electrolyte was introduced into the space between the two electrodes. A typical electrolyte contained LiI (0.05 M), I_2 (0.03 M), 4-*tert*-butylpyridine (TBP, 0.5 M), 1-propyl-3-methyl imidazolium iodide (PMII, 1.0 M) and guanidinium thiocyanate (GuNCS, 0.1 M) in a mixture of acetonitrile (CH_3CN, 99.9%) and valeronitrile (n-C_4H_9CN, 99.9%, v/v = 85/15).

Device characterization

The current–voltage characteristics were measured with a digital source meter (Keithley 2400, computer-controlled) with the device under one-sun AM-1.5 irradiation from a solar simulator (SAN-EI, XES-502S) calibrated with a standard silicon reference cell (VLSI standards, Oriel PN 91150V). The back-illuminated NT-DSSC devices were operated with rear illumination whereas the transparent NT-DSSC and NP-DSSC devices were illuminated from the front side. To determine the electron transport properties of the DSSC devices, we measured electrochemical impedance spectra (EIS) using an impedance-measuring unit (IM 6, Zahner) in a two-electrode design; the NT array film served as a working electrode and the Pt-coated FTO glass as a counter electrode at an applied bias of the open-circuit voltage under one-sun AM-1.5 irradiation. The frequency range was 0.05–1 MHz and the magnitude of the alternating potential was 10 mV. The EIS data were analyzed with an appropriate equivalent circuit using simulation software (Zahner).

Results and discussion

Fig. 1 illustrates the formation of a transparent NT array film to fabricate a front-illuminated NT-DSSC. The NT arrays (tube length 20 μm) as prepared were detached by secondary anodization (step 1 in Fig. 1).[20] During this process, a thin amorphous TiO_2 layer formed between the NT arrays and the Ti substrate with weak structural stability. After the film was rinsed with ethanol and dried in air, the NT film was easily peeled from the Ti substrate through surface tension (step 2 in Fig. 1).[10,27] The NT films were flat when wet but curled significantly during

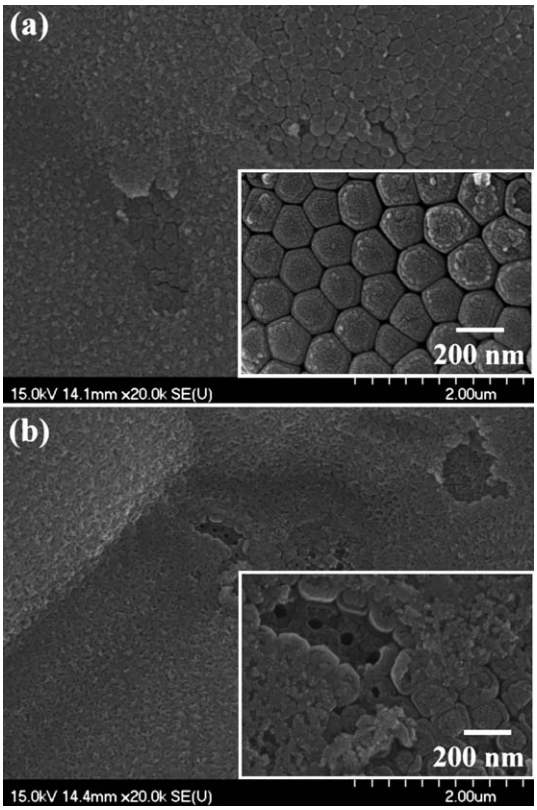

Fig. 2 SEM bottom-view images of NT arrays detached with secondary anodization at bias voltages (a) 20 and (b) 25 V for 4 h. The insets show the corresponding magnifications of the images.

evaporation, but secondary anodization is an excellent detaching method to prepare a non-curled NT film through elimination of the compressive stress at the barrier layer. We prepared NT array films as large as 6×6 cm^2 without curling, cracking or collapse. Fig. 2a and b shows SEM images (bottom view) of NT arrays detached with secondary anodization at bias voltages 20 and 25 V, respectively, each for anodization period of 4 h; the insets show the corresponding enlarged images. The newly grown amorphous TiO_2 structures adsorbed on the surface of the NT arrays at bias voltage 25 V, whereas a perfectly closed-end and flat-bottomed structure of the tubes was obtained on anodization at 20 V.

The detached NT arrays were transferred and attached onto a transparent FTO substrate coated with a thin layer of TiO_2 NP paste (thickness 2 μm). Of attaching methods of two types considered in the present work, the conventional face-up approach transferred the NT film in a parallel manner (step 3a in Fig. 1) whereas the proposed bottom-up approach transferred the film inverted onto the substrate (step 3b in Fig. 1). For the latter case, the closed-end structure of the NT arrays prohibits dye sensitization inside the nanotubes. To prevent the tubes from flaws or damage, we applied dry etching rather than wet chemical etching to open the enclosed tubes in a highly dense plasma reactor under BCl_3/Cl_2 (step 4 in Fig. 1). The periods of dry etching were selected to be 0 (as a reference), 30, 60, 90, 120 and 300 s; the corresponding SEM images are shown in Fig. 3a–f. The closed ends of the tubes were opened on increasing the period of etching to 60 s, but defects appeared under conditions of 120 and 300 s.

Fig. 4a and c shows top-view SEM images of transplanted NT films obtained with the upright and inverted approaches, respectively. Because the nanotubes feature a hollow conical columnar structure,[32] the average diameters of pore in the upright film is 100 nm, but 50 nm for the inverted film. Fig. 4b and d presents SEM images of side views (cross-sections) to inspect the interfaces for the upright and inverted films, respectively. For the upright film, the shape and thickness of the interfacial NP layer are more or less retained, and an apparent gap between the NT arrays and the NP layer was observed. The existence of gaps at the interface of the NT films might hinder

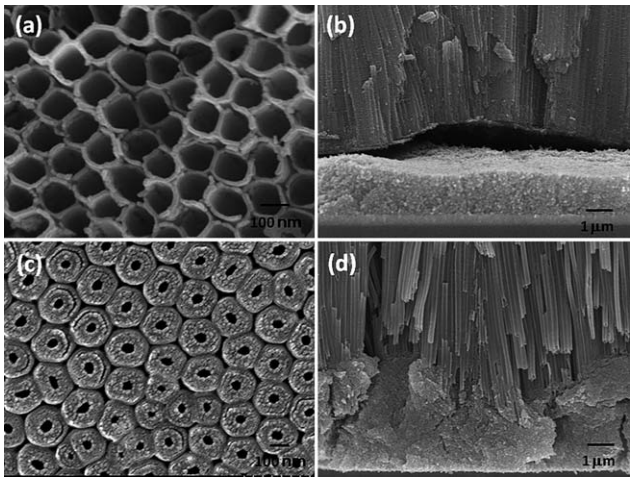

Fig. 4 SEM top-view images of (a) upright and (c) inverted attached NT arrays. The corresponding SEM side-view images of the interfaces between NT arrays and the NP paste layer are shown in (b) and (d).

electron transport and degrade substantially the device performance. For the inverted film, the NP paste entered the tubes to fill the interfacial gap, yielding a compactly adhered interface between the NT arrays and the FTO glass. These interfacial features of the films indicate that the NT-DSSC device based on the inverted approach might improve the efficiency of charge collection, and thereby improved cell performance relative to its upright counterpart.

The current–voltage characteristics of the corresponding DSSC devices are shown in Fig. 5. The corresponding photovoltaic parameters summarized in Table 1 demonstrate the current density at short circuit (J_{SC}/mA cm^{-2}), the voltage at open circuit (V_{OC}/V), the fill factor (FF), and the efficiency ($= J_{SC}V_{OC}FF/P_{in}$ with $P_{in} = 100$ mW cm^{-2}) of power conversion. The conventional back-illuminated NT-DSSC exhibits $J_{SC} = 9.56$ mA cm^{-2}, $V_{OC} = 0.76$ V and FF = 0.64, giving total efficiency 4.61% of power conversion at tube length 20 μm. To understand the contribution of the NP layer (2 μm) to the cell performance, we prepared a NP-DSSC as a control experiment. The reference NP-DSSC device shows $J_{SC} = 3.86$ mA cm^{-2},

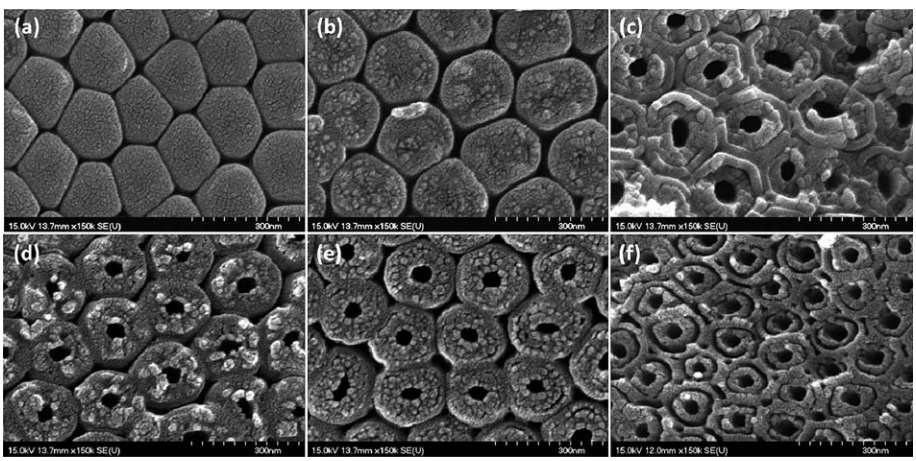

Fig. 3 SEM bottom-view images of (a) closed-end NT arrays, and those opened with dry etching in a highly dense plasma reactor under BCl_3/Cl_2 for (b) 30, (c) 60, (d) 90, (e) 120 and (f) 300 s.

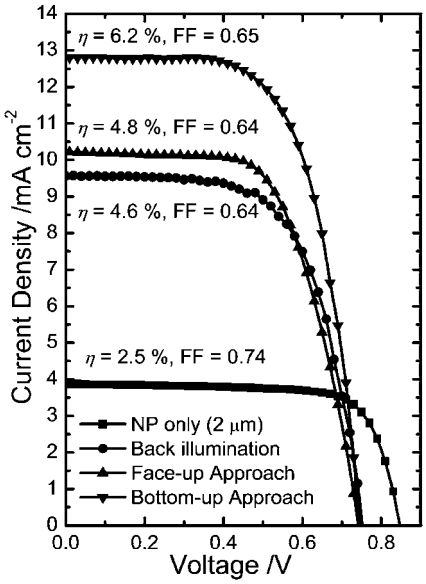

Fig. 5 Current–voltage characteristics of DSSC devices fabricated with (a) TiO_2 NP film (thickness 2 μm, ■), (b) NT arrays as prepared for back-illuminated device (●), (c) upright (face-up) attached NT arrays for front-illuminated device (▲) and (d) inverted (bottom-up) attached NT arrays for a front-illuminated device (▼) under simulated AM 1.5 solar illumination at 100 mW cm^{-2} with active area 0.16 cm^2.

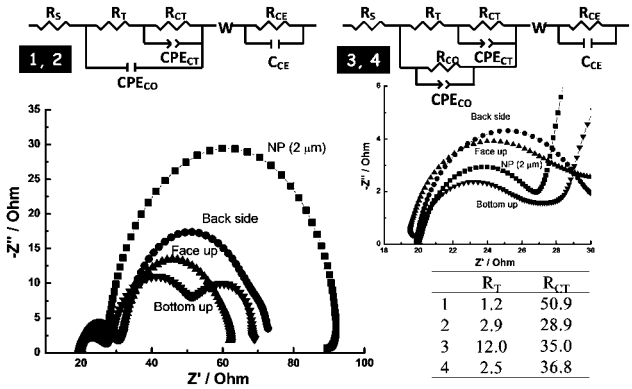

	R_T	R_{CT}
1	1.2	50.9
2	2.9	28.9
3	12.0	35.0
4	2.5	36.8

Fig. 6 Nyquist plots obtained from electrochemical impedance spectra (EIS) measured for corresponding DSSC devices shown in Fig. 5 under AM-1.5 illumination at open-circuit condition. Top models show the equivalent circuits used to fit the EIS results with series resistance (R_S), total transport resistance (R_T), charge-transfer resistance (R_{CT}) and capacitance (CPE_{CT}) at the TiO_2/electrolyte interface, film resistance (R_{CO}) and capacitance (CPE_{CO}) at the TiO_2/barrier layer interface, Warburg element (W) of electrolyte, and charge-transfer resistance (R_{CE}) and capacitance (C_{CE}) at the counter electrode interface.

$V_{OC} = 0.85$ V, FF = 0.74, and a total efficiency 2.45%. For the front-illuminated NT-DSSC devices, V_{OC} and FF of both upright and inverted devices are similar, but J_{SC} of the inverted device (12.78 mA cm^{-2}) is greater than that of the upright counterpart (10.21 mA cm^{-2}). This result is rationalized according to the effect of electron diffusion, for which the existence of gaps in the NT/FTO interface of the upright device results in impedance of electron transport to the collector.[22] The device performance of the inverted device outperforms that of the upright device because of superior charge collection of the former.

The amounts of dye loading are 243 and 178 nmol cm^{-2} for the upright and inverted devices, respectively, and those of the NP-only and the back-illuminated devices are 35 and 227 nmol cm^{-2}, respectively. Previously we found that J_{SC} increases upon increasing the amounts of dye loading when the tube length increases.[8,15] However, the larger J_{SC} of the inverted device compared with that of the upright device at the same tube length is not interpretable according to the effect of dye loading. Moreover, the dye loading of the upright device was similar to that of the back-illuminated one, but the front-illumination feature did not assist the upright device to generate an increased photocurrent because of the interfacial problem aforementioned. To understand the interfacial problems of the devices, we measured EIS; the corresponding results are shown in Fig. 6.

The impedance results were fitted according to the equivalent circuits shown on top of Fig. 6. The equivalent circuit elements describe the electron transport in a DSSC with typical physical meaning.[33,34] The transport resistances R_T/Ω at the TiO_2/substrate interface are 1.2, 2.9, 12.0 and 2.5 for DSSC devices based on NP, NT, upright and inverted structures, respectively. The NP-only device has a small R_T value because of its thin film. The transport resistance of the inverted transferred film is slightly smaller than that of the NT film as prepared without film transfer; the upright attached NT-DSSC device shows the largest transport resistance, indicating that electron diffusion was hindered by the cracks and gaps at the NT/NP interface. This result is consistent with the observed cell performance in that a smaller current density at short circuit was observed for the upright device than for the inverted device. Our results thus provide solid evidence for the transfer of inverted TNT arrays on a NP-coated TCO substrate to make a highly efficient NT-DSSC device with transparent front-side illumination.

Conclusion

A front-side illumination NT-DSSC was fabricated with detachment and transfer, involving secondary anodization

Table 1 Amount of dye-loading and corresponding photovoltaic parameters of DSSC devices under simulated AM-1.5 illumination (power 100 mW cm^{-2}) and active area 0.16 cm^2

TiO_2 electrodes	Film thickness/μm	Dye-loading/nmol cm^{-2}	J_{SC}/mA cm^{-2}	V_{OC}/V	FF	η (%)
NP/FTO	2	35	3.86	0.85	0.74	2.45
NT/Ti	20	227	9.56	0.76	0.64	4.61
Upright NT	2 + 20	243	10.21	0.74	0.64	4.84
Inverted NT	2 + 20	178	12.78	0.75	0.65	6.24

detachment, an inverted attached transfer and dry etching to open the closed ends. This approach facilely fabricates on a large scale transparent TiO_2 nanotube array without cracks that can firmly adhere to the surface of TCO glass coated with a thin layer of TiO_2 nanoparticles. The devices fabricated based on a conventional upright transfer exhibit much poorer performance than the inverted approach ($\eta = 4.84\%$ *vs.* 6.24%), indicating that cracks at the interface of NT arrays might hinder electron transport across the interface. Improved microstructure of the adhered interface in DSSC influences not only electron diffusion and charge collection but also the cell performance. Our results thus provide hope for further improvement of the cell performance for the front-illuminated NT-DSSC.

Acknowledgements

National Science Council of Taiwan and Ministry of Education of Taiwan, under the ATU program, provided support for this project.

References

1 B. O'Regan and M. Grätzel, *Nature*, 1991, **353**, 737.
2 M. K. Nazeeruddin, F. D. Angelis, S. Fantacci, A. Selloni, G. Viscardi, P. Liska, S. Ito, B. Takeru and M. Grätzel, *J. Am. Chem. Soc.*, 2005, **127**, 16835.
3 Y. Chiba, A. Islam, Y. Watanabe, R. Komiya, N. Koide and L. Han, *Jpn. J. Appl. Phys.*, 2006, **45**, L638.
4 F. Gao, Y. Wang, J. Zhang, D. Shi, M. Wang, R. Humphry-Baker, P. Wang, S. M. Zakeeruddin and M. Grätzel, *Chem. Commun.*, 2008, 2635.
5 F. Gao, Y. Wang, D. Shi, J. Zhang, M. Wang, X. Jing, R. Humphry-Baker, P. Wang, S. M. Zakeeruddin and M. Grätzel, *J. Am. Chem. Soc.*, 2008, **130**, 10720.
6 Y. Cao, Y. Bai, Q. Yu, Y. Cheng, S. Liu, D. Shi, F. Cao and P. Wang, *J. Phys. Chem. C*, 2009, **113**, 6290.
7 G. K. Mor, K. Shankar, M. Paulose, O. K. Varghese and C. A. Grimes, *Nano Lett.*, 2006, **6**, 215.
8 C.-C. Chen, H.-W. Chung, C.-H. Chen, H.-P. Lu, C.-M. Lan, S.-F. Chen, L. Luo, C.-S. Hung and E. W.-G. Diau, *J. Phys. Chem. C*, 2008, **112**, 19151.
9 L. Luo, C.-J. Lin, C.-Y. Tsai, H.-P. Wu, L.-L. Li, C.-F. Lo, C.-Y. Lin and E. W.-G. Diau, *Phys. Chem. Chem. Phys.*, 2010, **12**, 1064.
10 S. Rani, S. C. Roy, M. Paulose, O. K. Varghese, G. K. Mor, S. Kim, S. Yoriya, T. J. LaTempa and C. A. Grimes, *Phys. Chem. Chem. Phys.*, 2010, **12**, 2780.
11 M. Law, L. E. Greene, J. C. Johnson, R. Saykally and P. D. Yang, *Nat. Mater.*, 2005, **4**, 455.
12 K. Fujihara, A. Kumar, R. Jose, S. Ramakrishna and S. Uchida, *Nanotechnology*, 2007, **18**, 365709.
13 B. H. Lee, M. Y. Song, S.-Y. Jang, S. M. Jo, S.-Y. Kwak and D. Y. Kim, *J. Phys. Chem. C*, 2009, **113**, 21453.
14 K. Zhu, N. R. Neale, A. Miedaner and A. J. Frank, *Nano Lett.*, 2007, **7**, 69.
15 L.-L. Li, C.-Y. Tsai, H.-P. Wu, C.-C. Chen and E. W.-G. Diau, *J. Mater. Chem.*, 2010, **20**, 2753.
16 G. K. Mor, O. K. Varghese, M. Paulose and C. A. Grimes, *Adv. Funct. Mater.*, 2005, **15**, 1291.
17 G. K. Mor, K. Shankar, M. Paulose, O. K. Varghese and C. A. Grimes, *Nano Lett.*, 2006, **6**, 215.
18 O. K. Varghese, M. Paulose and C. A. Grimes, *Nat. Nanotechnol.*, 2009, **4**, 592.
19 J. H. Park, T. W. Lee and M. G. Kang, *Chem. Commun.*, 2008, 2867.
20 Q. W. Chen and D. S. Xu, *J. Phys. Chem. C*, 2009, **113**, 6310.
21 H. Park, W. R. Kim, H. T. Jeong, J. J. Lee, H. G. Kim and W. Y. Choi, *Sol. Energy Mater. Sol. Cells*, 2010, **95**, 184.
22 C. J. Lin, W. Y. Yu and S. H. Chien, *J. Mater. Chem.*, 2010, **20**, 1073.
23 B.-X. Lei, J.-Y. Liao, R. Zhang, J. Wang, C.-Y. Su and D.-B. Kuang, *J. Phys. Chem. C*, 2010, **114**, 15228.
24 C. Xu, P. H. Shin, L. Cao, J. Wu and D. Gao, *Chem. Mater.*, 2010, **22**, 143.
25 S. P. Albu, A. Ghicov, J. M. Macak, R. Hahn and P. Schmuki, *Nano Lett.*, 2007, **7**, 1286.
26 C.-J. Lin, W.-Y. Yu, Y.-T. Lu and S.-H. Chien, *Chem. Commun.*, 2008, 6031.
27 M. Paulose, H. E. Prakasam, O. K. Varghese, L. Peng, K. C. Popat, G. K. Mor, T. A. Desai and C. A. Grimes, *J. Phys. Chem. C*, 2007, **111**, 14992.
28 S. Norasetthekul, P. Y. Park, K. H. Baik, K. P. Lee, J. H. Shin, B. S. Jeong, V. Shishodia, E. S. Lambers, D. P. Norton and S. J. Pearton, *Appl. Surf. Sci.*, 2001, **185**, 27.
29 C.-C. Chen, W. C. Say, S.-J. Hsieh and E. W.-G. Diau, *Appl. Phys. A: Mater. Sci. Process.*, 2009, **95**, 889.
30 (*a*) S. Ito, P. Chen, P. Comte, M. K. Nazeeruddin, P. Liska, P. Péchy and M. Grätzel, *Progr. Photovolt.: Res. Appl.*, 2007, **15**, 603; (*b*) S. Ito, T. N. Murakami, P. Comte, P. Liska, C. Grätzel, M. K. Nazeeruddin and M. Grätzel, *Thin Solid Films*, 2008, **516**, 4613.
31 N. Papageorgiou, W. F. Maier and M. Grätzel, *J. Electrochem. Soc.*, 1997, **144**, 876.
32 C. C. Chen, W. D. Jehng, L. L. Li and E. W.-G. Diau, *J. Electrochem. Soc.*, 2009, **156**, C304.
33 Q. Wang, S. Ito, M. Grätzel, F. Fabregat-Santiago, I. Mora-Seró, J. Bisquert, T. Bessho and H. Imai, *J. Phys. Chem. B*, 2006, **110**, 25210.
34 F. Fabregat-Santiago, E. M. Barea, J. Bisquert, G. K. Mor, K. Shankar and C. A. Grimes, *J. Am. Chem. Soc.*, 2008, **130**, 11312.